AIAA JOURNAL
Vol. 40, No. 6, June 2002

Molecular Tagging Velocimetry Measurements in Supersonic Microjets

Walter R. Lempert,* Naibo Jiang,† Subin Sethuram,† and Mo Samimy‡
The Ohio State University, Columbus, Ohio 43210-1107

The application of acetone-based molecular tagging velocimetry (MTV) is demonstrated in sonic and supersonic jets produced by a 1-mm-exit-diameter nozzle. Measurements are performed in the static pressure range 1.3–53 mbar, with spatial resolution of approximately 10 μm. The statistical uncertainty (2σ) in velocity is found to be of order 6–10 m/s, approximately independent of flowfield pressure. Acetone laser-induced fluorescence temporal decay curves were also obtained, with 1/*e* lifetime found to range from ~ 200 ns at 1.3 mbar to less than 50 ns at 24 mbar. These relatively short lifetimes were nonetheless sufficient to obtain MTV data over the entire pressure range.

Introduction

In recent years, the interest in microdevices and systems has increased rapidly, and this trend is expected to continue for years to come. Gaseous flow through and within such devices is a principal consideration in many applications, and its understanding can be crucial for optimization of performance. Although the past 10 years has seen enormous progress in the general areas of microelectromechanical systems design and fabrication, detailed understanding of fundamental physical processes on these small scales is hampered by the lack of suitable quantitative measurement tools. In this paper, we demonstrate the use of acetone-based molecular tagging velocimetry (MTV) for quantitative measurement of velocity in high subsonic to supersonic jets issuing from micronozzles, such as those that might be employed for flow control and/or small satellite orbit maintenance.[1,2]

In general, microflows can be parameterized by the Knudsen number, $Kn = \lambda/\delta$, where λ is the molecular mean free path and δ is a characteristic flow length scale, which is typically a dimension of the device or system. Although there are some differences in the literature, the following is a typical breakdown of how the Knudsen number delineates the possible flow regimes[3]: $Kn < 0.001$, continuum flow; $0.001 < Kn < 0.1$, slip flow; $0.1 < Kn < 10$, transition flow; and $Kn > 10$, free-molecule flow.

Although there has been considerable recent progress in the development and application of quantitative velocimetry techniques in incompressible microflows, in both the liquid[4] and gas[5,6] phases, the extension to compressible flow has proven difficult. This paper focuses on demonstrating the capability of using acetone-based MTV to obtain quantitative velocity profiles in high subsonic to supersonic jets produced by nozzles with exit diameter of 1 mm and static pressures and temperatures of order 1.3–24 mbar and 250 K, respectively. These conditions correspond to a Knudsen number range from approximately 0.002 (low-density end of continuum regime) to 0.035 (slip regime).

MTV is a time-of-flight technique in which a laser is used to write a line (or set of lines) into a flow by means of an optical resonance with a suitable target tracer molecule. A particularly simple gas-phase MTV technique, originally demonstrated by Hiller et al.,[7] has recently been presented in more detail by Stier and Koochesfahani.[8] This approach utilizes biacetyl as a molecular tracer that, due to its relatively high vapor pressure at room temperature (on the order of millibars), can be readily seeded into gas-phase flows. Biacetyl has two strong absorption peaks centered at 270 and 430 nm. On absorption it exhibits relatively long-lived radiative emission (on the order of 0.1–1.0 ms) in nitrogen flows. (The phosphorescence is rapidly quenched in the presence of oxygen.) Velocity is determined by imaging the laser-induced phosphorescence from the initially excited line a suitable time delay after excitation. The measurement requires only a single, modest, power-pulsed near UV laser (on the order of 1 mJ per line) for the tagging step, and a gatable, intensified charge-coupled device (CCD) camera for the subsequent imaging (or interrogation) step.

At the suggestion of Manooch Koochesfahani in a private communication, we have performed the MTV measurements to be presented in this paper using acetone, which has a higher vapor pressure than biacetyl and is somewhat easier to work with. (Although biacetyl is not toxic, the human nose is quite sensitive to it, necessitating some additional experimental care.) Although acetone has been used extensively as a tracer for scalar mixing studies,[7–13] this paper reports, to our knowledge, the first use of acetone as a molecular tracer for quantitative velocimetry. Acetone photophysics is similar in many respects to biacetyl, except that it is excited in the wavelength range of approximately 230–340 nm. This absorption band is well matched to the outputs of either the Nd:YAG (fourth harmonic at 266 nm) or XeCl (308-nm) lasers.

MTV is similar, in many respects, to what is termed flow tagging velocimetry.[14] Flow tagging utilizes a pair of excitation lasers, one of which drives the tagged molecules into an excited, metastable electronic and/or vibrational state, or induces a photochemical reaction. After a suitable time delay, standard planar laser fluorescence imaging techniques, employing a second laser, are used to interrogate the displacement of the initially tagged fluid elements. Gas-phase oxygen- and ozone-based flow tagging have recently been reviewed by Miles et al.[15] and Pitz et al.,[16] respectively. Application of MTV to incompressible flow has recently been reviewed by Koochesfahani et al.,[17] who employed long-life time supramolecules, and Lempert and Harris,[18] who employed caged dye photoactivated fluorophores.

Experimental Approach

Figure 1 shows a schematic drawing of the essential features of the experimental apparatus. The complete facility consists of a vertically oriented volatile vapor seeding cylinder, a $25.4 \times 25.4 \times 101$ mm rectangular test cell with four-sided optical access, a 5-liter cylindrical dump tank, and a 1000-liter/min vacuum pump. To minimize interference from window fluorescence, suprasil quartz was employed, which exhibits exceedingly low levels of fluorescence.

Presented as Paper 2001-0244 at the AIAA 39th Aerospace Sciences Meeting, Reno, NV, 8–11 January 2001; received 14 March 2001; revision received 17 September 2001; accepted for publication 27 September 2001.

*Associate Professor, Departments of Mechanical Engineering and Chemistry. Associate Fellow AIAA.
†Graduate Student, Department of Mechanical Engineering.
‡Professor, Department of Mechanical Engineering. Associate Fellow AIAA.

Acetone-seeded nitrogen test gas is delivered by bubbling dry nitrogen from a standard laboratory cylinder through the seeding chamber to the nozzle. (The mole fraction of acetone has not been determined.) The test gases are delivered at ambient room temperature. Nozzles are inserted into the test cell by means of standard fittings. As an initial test case for molecular tagging, a 1-mm-i.d. straight cylindrical tube has been employed as the nozzle. A pressure tap was drilled into the nozzle, at a location 1–2 mm from the exit. A second pressure tap is located in the test section, to provide a measurement of the ambient back pressure. For the work to be presented in this paper, the jet was operated with an exit pressure in the range ~1.3–53 mbar. The facility pumping speed was adjusted by partial closing of a valve located between the exit of the dump tank and the pump. By suitable combination of stagnation pressure, flow rate, and pumping speed, the nozzle could be operated in flow regimes ranging from pressure matched ($P_{exit} = P_{ambient}$) to highly underexpanded (from P_{exit} up to $10P_{ambient}$).

Single lines were written into the flow at a location ~$\frac{3}{4}$ mm from the nozzle exit by focusing the fourth harmonic output (at 266 nm) from a mini, pulsed Nd:YAG laser using a 100-mm-focal-length planoconvex lens. The individual pulse energy was approximately 8 mJ, and the pulse duration was approximately 5 ns. Displaced images were captured using an 18-mm microchannel plate intensified CCD (ICCD) camera and a standard Nikon 50-mm $\mathcal{F}/1.8$ 35-mm format camera lens. Image magnification of either ~2:1 or 4:1 was accomplished by inclusion of a suitable number of lens extension tubes. The effective spatial resolution of the measurement, although not studied in detail, is, in principal, determined by the combination of the ICCD resolution (~25 lp/mm) and the lens magnification. As an example, at 4:1 magnification, a spatial resolution of 40 μm (or 25 lp/mm) in the image plane (i.e., at the plane of the image intensifier) maps into 10 μm in the object plane, that is, the flowfield. This, in turn, maps into approximately one CCD pixel, assuming a pixel size of ~20 μm and a 2:1 image relay lens between the intensifier and the 10-mm format CCD sensor. However, as will be discussed in more detail, realizable spatial resolution, particularly at low density, can be constrained by mass diffusion and collection solid angle.

For all measurements to be presented in this paper, signals were averaged for 5–10 s, at a laser repetition rate of 10–20 Hz. Images obtained at two times and four times magnification have corresponding spatial scales of ~14 and 9 μm/pixel, respectively.

Results

Velocity Images

Figures 2a–2c show a representative set of acetone MTV interrogation images obtained under pressure matched conditions with $P_{exit} = P_{ambient} = 2.6, 5.2$, and 7.9 mbar, respectively. In all cases the line was written ~$\frac{3}{4}$ mm downstream from the jet exit. The interrogation delay time was 350 ns for Fig. 2a and 400 ns for Figs. 2b and 2c. The approximate initial tagging position is illustrated in Fig. 2d, which shows a line 10 ns after tagging. In all cases, the images were obtained using the 2:1 magnification system, and the displayed field of view is 5 × 8 mm. As will be described in more detail in the next section, least-squares fits indicate centerline velocities of 248, 307, and 344 ± 8–10 m/s (2σ), respectively, for Figs. 2a–2c.

Also evident in the images of Fig. 2 is the considerable effect of mass diffusion. The increasing thickness of the interrogated line with decreasing pressure is qualitatively consistent with the expected linearly increasing coefficient of mass diffusion.

Figure 3 shows a velocity image obtained with the jet operated under highly underexpanded conditions (P_{exit} ~ 53 mbar and $P_{ambient}$ ~ 9.2 mbar) with a time delay of 300 ns. The velocity profile

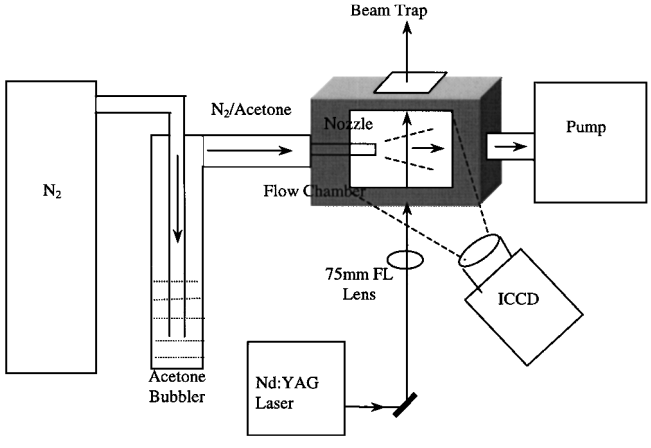

Fig. 1 Schematic diagram of apparatus.

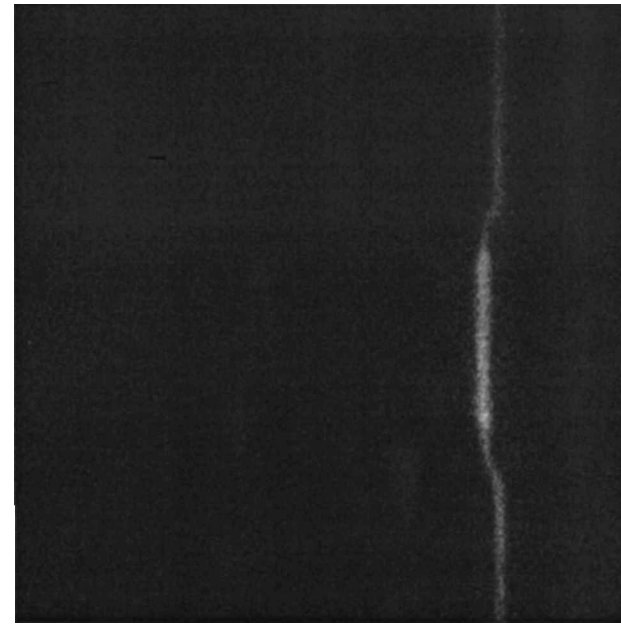

Fig. 3 Representative MTV image for nozzle operated under highly underexpanded conditions: P_{exit} ~ 53 mbar and $P_{ambient}$ ~ 9 mbar.

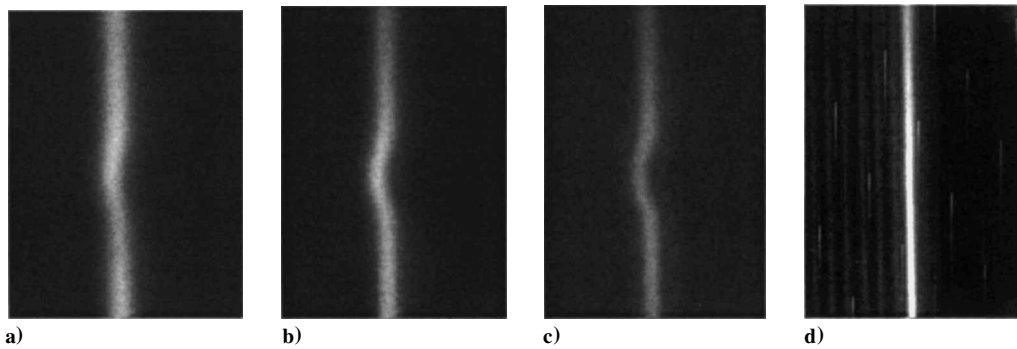

Fig. 2 Representative MTV images obtained under near pressure matched conditions at a) 2.6 mbar b) 5.2 mbar, and c) 7.9 mbar; d) right-hand image obtained 10 ns after tagging at 7.9 mbar shows approximate initial tagging position, which is ~ 0.75 mm downstream from nozzle exit. Flow direction is from right to left. Time delay is 350 ns for 2.6-mbar image and 400 ns for 5.2- and 7.9-mbar images.

is clearly more flat topped, and intensity variation along the line is quite apparent. As will be described, the interrogated signal intensity is strongly influenced by the pressure dependence of the fluorescence lifetime. In addition, the magnitude of the centerline velocity and density is expected to significantly change with an increasing ratio of nozzle exit pressure to ambient pressure and the streamwise distance from the nozzle exit.

Velocity Data

Quantitative velocity data are obtained using a simple least-squares fitting procedure,[19] similar to that which has been described in previous flow tagging studies.[20] Note that the use of a single MTV line limits the measurement to the component of velocity normal to the initial tagging line. For all data presented in this paper, the measured component of velocity is along the jet/nozzle axis, which is the principal flow axis. Additionally, there is some potential inherent ambiguity in the transverse location of the interrogated fluid element. Strategies for addressing this issue, including grid writing[21] and associated image processing,[22,23] and direct Lagrangian frame data/theory comparison,[24] are discussed in detail in Ref. 25. With this constraint, the velocity is assumed to be given by the ratio of the displacement to the elapsed time and represents, therefore, a spatial and temporal average. Figure 4 shows the digitized gray scale pixel intensity from a single horizontal slice of the image in Fig. 3, as well as from the zero delay image (not shown, but essentially identical to Fig. 2d). Also shown in Fig. 4 are least-squares fits to assumed Gaussian and Lorentzian spatial profiles, respectively, for the interrogation and tagging data. (For reasons not entirely clear, the tagging data are better represented by a Lorentzian profile, whereas the interrogation data are better represented by the expected, mass diffusion dominated Gaussian profile.) The selected slice is from near the flow centerline and the measured centerline flow velocity is 661 ± 10 m/s (2σ). Figure 5 shows a similar set of digitized centerline slices obtained from the data of Figs. 2c and 2d. The corresponding velocity is 344 ± 10 m/s, which is slightly greater than the predicted Mach 1 centerline velocity of 320 m/s. Finally, Fig. 6 shows fits from data obtained under near pressure matched conditions at 1.3 mbar exit pressure, employing the four-times image magnification system. The velocity is 200 ± 6.6 m/s (2σ), indicating that the flow has become subsonic throughout the entire radial profile of the jet.

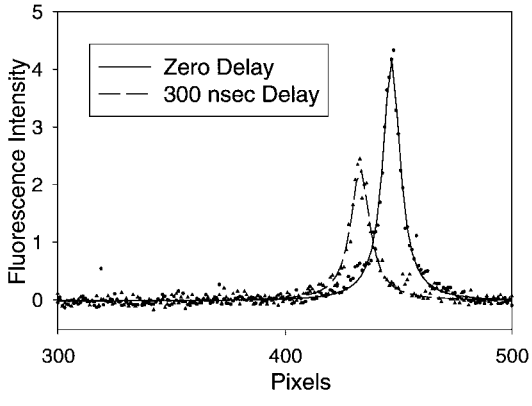

Fig. 4 Single horizontal slice of gray scale intensity (left-hand symbols) and least squares fit (left-hand dashed curve) from near centerline of underexpanded flow image shown in Fig. 3; curve and symbols on right are from initial tagging line, and spatial scale is ~ 14 μm/pixel.

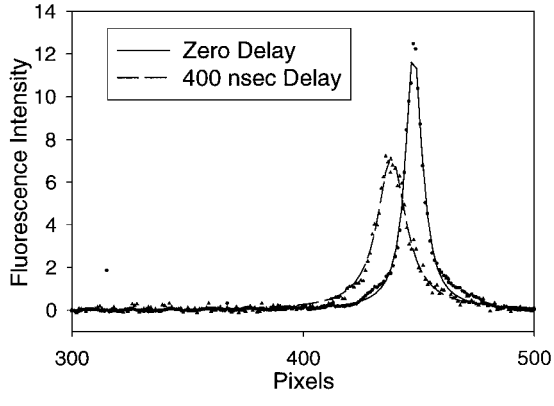

Fig. 5 Similar to Fig. 4, except that data are from 7.9 mbar near pressure matched MTV images of Fig. 2c (left) and Fig. 2d (right); spatial scale is ~ 14 μm/pixel.

Discussion

Velocity Accuracy

All velocity accuracy values quoted in this work are derived from the rms sum of the statistical uncertainties in the line center positions of the zero delay (tagging) and displaced (interrogation) images, as determined by the least-squares curve fits (specifically, from the diagonal elements of the covariance matrix[19]). This assumes that the residual between the best-fit curves and the experimental data points is due, entirely, to statistical scatter in the data. For the signal-to-noise ratios S/N in the experimental images collected for this work, the statistical uncertainty is typically found to be of the order 2–3% of the full width at half maximum of the interrogated line segment. This was found to be only a modest function of S/N ratio. Note also that the contribution to the uncertainty due to the uncertainty in time is negligible.

Inspection of Figs. 4–6 illustrates qualitatively the effect of mass diffusion on the interrogated line profiles, which is significant at the characteristically low static pressures employed in this work. Quantitatively, the line width (half width at half maximum) of the tagged fluid element ω should increase according to the following equation[26]:

$$\omega^2 = 4\Delta t D_m \ln(2) + \omega_0^2 \tag{1}$$

where Δt is the time interval between tag and interrogation, ω_0 is the initial thickness of the tagged fluid element (dictated by the focused laser beam thickness), and D_m is the coefficient of mass diffusion. For the case of binary diffusion of one species A into another, B, this coefficient is approximated by

$$D_{m,AB} = 0.0018583 \frac{\sqrt{T^3(1/M_A + 1/M_B)}}{P\sigma_{AB}^2 \Omega_{m,AB}} \tag{2}$$

where M_A and M_B are the molecular masses of the species, σ_{AB} is the Lennard–Jones length parameter (in angstroms), T is the temperature (in degrees Kelvin), P is the pressure (in atmospheres), and $\Omega_{m,AB} = KT/\varepsilon_{AB}$, where ε_{AB} is the Lennard–Jones well depth parameter.[27] Using data tabulated in Ref. 27, we predict a value of $D_{m,AB} \sim -0.093$ cm^2/s at 1 bar and 300 K. However, preliminary attempts to verify this were unsuccessful. Whereas linewidths extracted from MTV interrogated images scaled qualitatively as the square root of elapsed time, quantitatively inferred diffusion coefficients, scaled to 1 bar, were found to be too high by as much as a

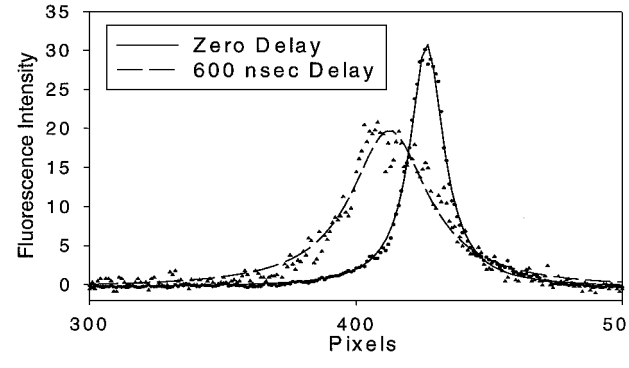

Fig. 6 Gray scale intensity and least-squares fits to pressure matched data obtained at 1.3 mbar static pressure using higher magnification four-times imaging configuration; spatial scale is ~ 9 μm/pixel.

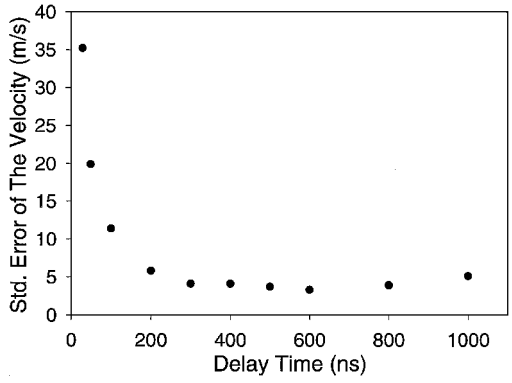

Fig. 7 Statistical uncertainty in velocity as a function of time delay for single slice of pressure matched MTV data obtained at 1.3-mbar static pressure; minimum uncertainty (1σ) is 3.3 m/s at 600-ns time delay.

factor of two. Although this needs to be studied in more detail, there are several potential sources of error, including static pressure measurement inaccuracy, flow unsteadiness, and, as will be discussed, possible photodissoication of acetone to lighter fragments and/or insufficient depth of field in the imaging system.

Nonetheless, the primary significance of Eqs. (1) and (2) is that, at low densities, characteristic of slip and transition flows, mass diffusion (and, therefore, interrogated fluid element thickness) significantly influences the realizable velocity accuracy. Fortunately, because ω increases as only the square root of time, accuracy can be increased, at least to some extent, by increasing the time delay between tag and interrogation. Figure 7 shows a plot of σ_v as a function of time delay for pressure matched flow at 1.3 mbar, obtained from single horizontal slices of data, similar to those of Figs. 4–6. Note that the velocity uncertainty decreases rapidly as Δt is increased from ~50 to 300 ns. A minimum value of 3.3 m/s (1σ) is reached at 600 ns, after which the uncertainty increases slowly, due, primarily, to a drop in signal-to-noise ratio in the interrogated images. Note that, for this case, the mean flow velocity is 200 m/s, so that the best case accuracy corresponds to a fractional uncertainty of ~3.5% (2σ). The total fluid displacement required to achieve this accuracy is ~120 μm. Although a comprehensive study has not yet been performed for other pressure conditions, it is anticipated that the results will be similar. In particular, as will be described in the next section, decreased mass diffusion at higher pressure is approximately balanced by decreased fluorescence lifetime (and, therefore, displacement), resulting in velocity uncertainty that is in the range 6–10 m/s, nearly independent of pressure.

Spatial Resolution

The spatial resolution of ICCD cameras has been discussed in detail by Paul,[28] including a detailed analysis of the effect of sheet thickness on resolution in planar laser-induced fluorescence imaging. Although somewhat of a simplification, the criteria described in Ref. 28 can be qualitatively understood by consideration of what is known in geometrical optics as the depth of field δa, which is typically defined as

$$\delta a = 2\lambda(a/D)^2 \tag{3}$$

where a is the on-axis distance from the object to the lens, D is the lens diameter, λ is the wavelength of light, and δa is the maximum $\pm$ displacement of the object from the true focus position, based on the Rayleigh quarter-wave criterion (see Ref. 29). This allows one to develop a criterion, albeit a qualitative one, for assuring that degradation of spatial resolution due to object thickness is minimal. For example, for $\delta a = \pm 50$ μm (or greater) and $\lambda = 0.5$ μm, a/D must be ~7 (or greater). Most of the images presented in this paper were collected with $a/D \sim 3$, which implies some spatial resolution degradation, particularly at low pressure where, as discussed earlier, diffusion significantly increases the tagged fluid element thickness. We plan to study this in more detail in the near future.

Acetone Fluorescence Characteristics

Acetone fluorescence has been utilized extensively as a tracer for scalar mixing measurements, particularly in combustion studies.[9–13] It is now generally accepted[12] that on single photon excitation to the S_1 excited electronic state, fluorescence decay occurs through one of four mechanisms:

1) The first mechanism is fluorescence decay to the ground state (with radiative lifetime of ~1 μs).

2) The second mechanism is rapid (~nanoseconds) collisionless intersystem crossing to an intermediate mixed state with singlet and triplet character.

3) At pressures exceeding a few millibar, this mixed state is rapidly collisionally quenched to a long-lived (~milliseconds) triplet excited state.

4) Finally, also at low pressure, collsional transfer to and subsequent fluorescence decay from what is known as the hot triplet state.[30,31] It is processes 2 and 3 that, at high pressure, provide the basis for scalar mixing studies because they have the effect, while limiting the signal, of creating a pressure independent fluorescence quantum yield. In this way, the detected signal becomes directly proportional to acetone density.

At lower pressure, however, it appears that radiative decay from the mixed and hot triplet states becomes significant. Although these states have not been studied in enormous detail, it is clear that at extremely low pressures (order 10^{-6} bar), the lifetimes can be as long as tens of microseconds, depending on excitation wavelength.[30,31] Although, to our knowledge, the radiative properties of acetone have not been studied in detail in the pressure and excitation wavelength regime used in this work, it appears that the MTV measurements presented in this paper are taking advantage of a lifetime intermediate between that of the first singlet (5 ns) and the triplet (milliseconds) states. This hypothesis is supported by the data of Fig. 8, which show the normalized fluorescence intensity as a function of time delay for pressures ranging between 1.3 and 24 mbar. Again, these data were extracted from least-squares fits to single horizontal slices of pressure-matched flow data. The intensity axis is the product of the peak intensity and the spatial width, which is proportional to the spatially integrated intensity. Note that the $1/e$ fluorescence decay decreases from ~200 ns at 1.3 mbar to ~50 ns at 24 mbar. Whereas it is not obvious from Fig. 8, it was found empirically that usable image data could typically be obtained for time delays corresponding to drops in intensity of $\sim 1/e^4$ (or ~2% of peak). Additionally, by combination of the data of Figs. 7 and 8, it can be seen that the minimum velocity uncertainty is obtained at time delays corresponding to between $1/e^2$ and $1/e^3$ intensity decay. Inspection of Fig. 8 also shows that the intensity does not appear to decay as a single exponential, indicating the presence of competing processes. Although this is reasonable, it has not yet been studied in detail.

Note that we have not verified the absence of acetone photodissociation, which, under some conditions, is known to occur.[32] In

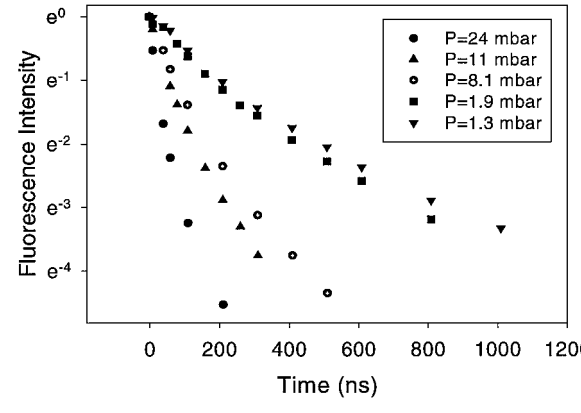

Fig. 8 Acetone fluorescence decay as a function of time for pressure matched flow at static pressures between 1.3 and 24 mbar; usable MTV images were obtained for time delays corresponding to approximately $1/e^4$ decay.

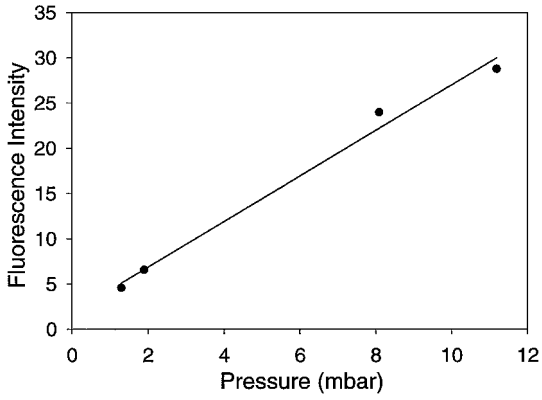

Fig. 9 Acetone fluorescence intensity at $t = t_0$ as a function of pressure.

particular, significant fragmentation would influence both the fluorescence lifetime and mass diffusion. We plan detailed spectroscopic studies in the near future.

Finally, Fig. 9 shows the intensity of the initially tagged fluid as a function of pressure in the range 1.3–10.5 mbar for single slices of pressure-matched flow data. These data were obtained using an intensifier gate width of 20 ns, which is much less than the $1/e$ decay time in this pressure range. Note that the signal is approximately linear. This suggests that the technique has the potential to be used to obtain density field data, which, when combined with velocity, will yield momentum flux and velocity–density correlation. Whereas this type of combined scalar–vector MTV measurement has been successfully demonstrated in the liquid phase,[21] extension to the gas phase will require knowledge of the temperature dependence of the acetone phosphorescence quantum yield, similar to that which has been determined for fluorescence.[12]

Conclusions

We have demonstrated the applicability of acetone-based MTV to quantitative measurement of velocity in supersonic flows at micrometer-scale resolution. Measurements have been obtained in the flow produced by a 1-mm-diam straight nozzle, in a static pressure range between approximately 1.3 and 53 mbar and velocity range from high subsonic to supersonic.

Least-squares fits were performed to provide an estimate of the statistical uncertainty in the experimental velocity data. It was found that mass diffusion significantly influences the realizable accuracy and spatial resolution, due to broadening of the spatial profile of the interrogated images. Velocity accuracy was found to be of the order 6–10 m/s (2σ), approximately independent of pressure in the range 1.3–24 mbar. Whereas diffusion broadening decreases with increasing pressure, the fluorescence lifetime and, therefore, the usable time delay between tag and interrogation, also decreases, resulting in an approximate cancellation of effects.

Acetone fluorescence decay curves were obtained in the pressure range 1.3–24 mbar. A very significant pressure quenching was observed, with the $1/e$ fluorescence lifetime decreasing from approximately 200 ns at 1.3 mbar to approximately 50 ns at 24 mbar. This implies the possibility that MTV measurements at low pressure are taking advantage of previously reported mixed singlet-triplet and/or hot triplet intermediate lifetime excited electronic states.

Acknowledgments

This work was supported by the U.S. Air Force Office of Scientific Research program in Unsteady Aerodynamics and Hypersonics, Steven Walker, Technical Monitor. The authors would like to thank Manooch Koochesfahani of Michigan State University for many helpful discussions. The assistance of Samuel Merriman, Adam Christian, and Brett Kowalczyki, who assembled the flow facility, is also acknowledged.

References

[1]Bayt, R., and Breuer, K., "Systems Design and Performance of Hot and Cold Supersonic Microjets," AIAA Paper 2001-0721, Jan. 2001.

[2]Ketsdever, A. D., Green, A. A., and Muntz, E. P., "Momentum Flux Measurements from Under Expanded Orifices: Applications for Microspacecraft Systems," AIAA Paper 2001-0502, Jan. 2001.

[3]Gad-el-Hak, M., "The Fluid Mechanics of Microdevices," *Journal of Fluids Engineering*, Vol. 121, March 1999, pp. 5–33.

[4]Paul, P. H., Garguilo, M. G., and Rakestraw, D. J., "Imaging of Pressure- and Electrokinetically Driven Flows Through Open Capillaries," *Analytical Chemistry*, Vol. 70, No. 13, 1998, pp. 2459–2467.

[5]Santiage, J. G., Werely, S. T., Meinhart, C. D., Beebe, D. J., and Adrian, R. J., "A Particle Image Velocimetry System for Microfluidics," *Experiments in Fluids*, Vol. 25, No. 4, 1998, pp. 316–319.

[6]Werely, S. T., Gui, L., and Meinhart, C. D., "Flow Measurement Techniques for the Microfrontier," AIAA Paper 2001-0243, Jan. 2001.

[7]Hiller, B., Booman, R. A., Hassa, C., and Hanson, R. K., "Velocity Visualization in Gas Flows Using Laser-Induced Phosphorescence of Biacetyl," *Review of Scientific Instruments*, Vol. 55, No. 12, 1984, pp. 1964–1997.

[8]Stier, B., and Koochesfahani, M. M., "Molecular Tagging Velocimetry (MTV) Measurements in Gas Phase Flows," *Experiments in Fluids*, Vol. 26, No. 4, 1999, pp. 297–304.

[9]Lorenzo, A., Yip, B., and Hanson, R. K., "Acetone: A Tracer for Concentration Measurements in Gaseous Flows by Planar Laser-Induced Fluorescence," *Experiments in Fluids*, Vol. 13, No. 6, 1992, pp. 369–376.

[10]Bryant, R. A., Donbar, J. M., and Driscoll, J. F., "Acetone LIF for Flow Visualization at Low Temperatures Below 300 K," AIAA Paper 97-0156, Jan. 1997.

[11]Hiltner, J., and Samimy, M., "The Impact of Injection Timing on In-Cylinder Fuel Distribution a Natural Gas Powered Engine," Society of Automotive Engineers, SAE Paper 971708, May 1997.

[12]Thurber, M. C., Grisch, F., Kirby, B. J., Votsmeier, M., and Hanson, R. K., "Measurements and Modeling of Acetone Laser-Induced Fluorescence with Implications for Temperature-Imaging Diagnostics," *Applied Optics*, Vol. 37, No. 21, 1998, pp. 4963–4978.

[13]Ritchie, B. D., and Seitzman, J. M., "Quantitative Acetone PLIF in Two-Phase Flows," AIAA Paper 2001-0414, Jan. 2001.

[14]Miles, R., Cohen C., Connors J., Howard P., Huang, S., Markovitz, E., and Russell, G., "Velocity Measurements by Vibrational Tagging and Fluorescent Probing of Oxygen," *Optics Letters*, Vol. 12, No. 11, 1987, pp. 861–863.

[15]Miles, R. B., Grinstead, J., Kohl, R. H., and Diskin, G., "The RELIEF Flow Tagging Technique and Its Application in Engine Testing Facilities and for Helium–Air Mixing Studies," *Measurement Science and Technology*, Vol. 11, No. 9, 2000, pp.1272–1281.

[16]Pitz, R. W., Wehrmeyer, J. A., Ribarov, L. A., Oguss, D. A., Btliwala, F., DeBarber, P. A., Deusch, S., and Dimotakis, P. E., "Unseeded Molecular Flow Tagging in Cold and Hot Flows Using Ozone and Hydroxyl Tagging Velocimetry," *Measurement Science and Technology*, Vol. 11, No. 9, 2000, pp.1259–1271.

[17]Koochesfahani, M., Cohn, R., and MacKinnon, C., "Simultaneous Whole-Field Measurements of Velocity and Concentration Fields Using a Combination of MTV and LIF," *Measurement Science and Technology*, Vol. 11, No. 9, 2000, pp.1289–1300.

[18]Lempert, W. R., and Harris, S. R., "Flow Tagging Velocimetry Using Caged Dye Photoactivated Fluorophores," *Measurement Science and Technology*, Vol. 11, No. 9, 2000, pp. 1251–1258.

[19]Bevington, P. R., *Data Reduction and Error Analysis for the Physical Sciences*, McGraw–Hill, New York, 1969, pp. 153–156.

[20]Noullez, A., Wallace, G., Lempert, W., Miles, R. B., and Frisch, U. J., "Transverse Velocity Increments in Turbulent Flow Using the RELIEF Technique," *Journal of Fluid Mechanics*, Vol. 339, June 1997, pp. 287–307.

[21]Gendrich, C. P., Koochesfahani, M. M., and Nocera, D. G., "Molecular Tagging Velocimetry and Other Novel Applications of a New Phosphorescent Supramolecule," *Experiments in Fluids*, Vol. 23, No. 5, 1997, pp. 361–372.

[22]Hill, R. B., and Klewicki, J. C., "Data Reduction Methods for Flow Tagging Velocity Measurements," *Experiments in Fluids*, Vol. 20, No. 3, 1996, pp. 142–152.

[23]Gendrich, C. P., and Koochesfahani, M. M., "A Spatial Correlation Technique for Estimating Velocity Fields Using Molecular Tagging Velocimetry (MTV)," *Experiments in Fluids*, Vol. 22, No. 1, 1996, pp. 67–77.

[24]Harris, S. R., Miles, R. B., and Lempert, W. R., "Comparisons Between Flow Tagging Measurements and Computations in a Complex Rotating Flow," AIAA Paper 97-0852, Jan. 1997.

[25]Lempert, W. R., and Harris, S. R., "Molecular Tagging Velocimetry," *Flow Visualization—Techniques and Examples*, edited by A. J. Smits and T. T. Lim, 1st ed., Imperial College Press, London, 2000, pp. 73–92.

[26]Bronwell, A., *Advanced Mathematics in Physics and Engineering*, McGraw–Hill, New York, 1953, pp. 263–266.

[27]Bird, R. B., Stewart, W. E., and Lightfoot, E. N., *Transport Phenomena*, Wiley, New York, 1962, pp. 508–513.

[28]Paul, P. H., "The Application of Intensified Array Detectors to Quantitative Planar Laser-Induced Fluorescence Imaging," AIAA Paper 91-2315, June 1991.

[29]Levi, L., *Applied Optics—A Guide to Optical System Design/Volume I*, Wiley, New York, 1968, pp. 468, 469.

[30]Copeland, R. A., and Crosley, D. R., "Radiative, Collisional, and Dissociative Processes in Triplet Acetone," *Chemical Physics Letters*, Vol. 115, No. 4, 1985, pp. 362–368.

[31]Greenblatt, G. D., Ruhman, S., and Haas, Y., "Fluorescence Decay Kinetics of Acetone Vapor at Low Pressures," *Chemical Physics Letters*, Vol. 112, No. 3, 1984, pp. 200–206.

[32]Emrich, M., and Warneck, P., "Photodissociation of Acetone in Air: Dependence on Pressure and Wavelength. Behavior of the Excited Singlet State," *Journal of Physical Chemistry A*, Vol. 104, No. 37, 2000, pp. 9436–9442.

R. P. Lucht
Associate Editor